

Chapter 3: Techniques of Synthesis & Characterization of ZnO Nanostructures

3.1 Introduction

Among physical vapor deposition techniques thermal evaporation (TE) is the one with the longest standing tradition. However, during the last 30 years of booming semiconductor industry which involves a great deal of thin film technology, deposition techniques like CVD (chemical vapor deposition) or sputtering which often offer unquestionable advantages have been developed to perfection and TE has largely been replaced in production lines. On the laboratory scale, due to their simplicity, techniques like PLD (pulsed laser deposition) or sputtering are much more promising to realize fast results. Consequently, when the new superconductors emerged only a handful of research groups like Berberich (1988), Terashima (1988), Kwo (1989), Prakash (1990), and Chew (1990) performed deposition trials based on TE. However, as time went by it became clear that the performance of the various deposition methods strongly depends on material issues as well as economic aspects. With progressive commercialization, cost effective volume production and reproducibility became the driving forces and the intrinsic advantages of TE turned on the scales.

3.2 Preparation of ZnO Thin Films

To study the electrical and optical properties of ZnO nanostructures, thin films are generally used. The properties of thin films of the material are different from those of the bulk due to the presence of several additional factors such as discontinuities, structural defects, grain growth and phase changes in thin films. These additional factors in thin films are induced due to various deposition parameters [1]. Non crystalline thin films of the materials can be prepared by using different methods. The methods used to deposit thin films may be divided into two main groups, physical and chemical. Some of the physical methods for thin films deposition are vacuum evaporation [2-5], electron-beam evaporation [6], flash-evaporation [7], RF sputtering [8] multi-source evaporation, ion-beam evaporation [9] laser-beam evaporation, diode or triode sputtering, resistive evaporation, reactive evaporation and exploding wire evaporation. Some chemical methods of thin films deposition are anode electrolytic deposition [10], chemical bath deposition [11], cathode electrolytic deposition [12], chemical vapour deposition and plasma-enhanced chemical vapour deposition [13, 14] In the present work, physical vapor condensation method has been used for the preparation of ZnO nanostructures thin film. In this method, the source material is Zn powder (99.999 % pure), which is evaporated in the presence of oxygen and argon gases present in the chamber. Initially, small quantity of Zn powder has been kept in a molybdenum boat and the chamber is evacuated to a vacuum of the order of 10^{-6} Torr. After attaining this vacuum, the gases (oxygen and argon) are purged in to the chamber. The pressure of these gases is kept fixed at 16 mbar and 4 mbar respectively. Evaporated material is deposited on LN2 cooled glass substrate. The nanoparticles of ZnO are deposited on the glass substrate and also collected in the powder form by scratching it from the substrate.

3.3 Deposition System

Figure 3.1 shows schematic diagram of evaporation chamber. It consists of substrate holder, heating source, vacuum pump. The vacuum system consists of a vacuum chamber which is of cylindrical form of diameter around 350 mm, made up of stainless steel and electro-polished for good vacuum performance. The cylinder is having a substrate-loading window of 150 mm diameter and can be used as view port.

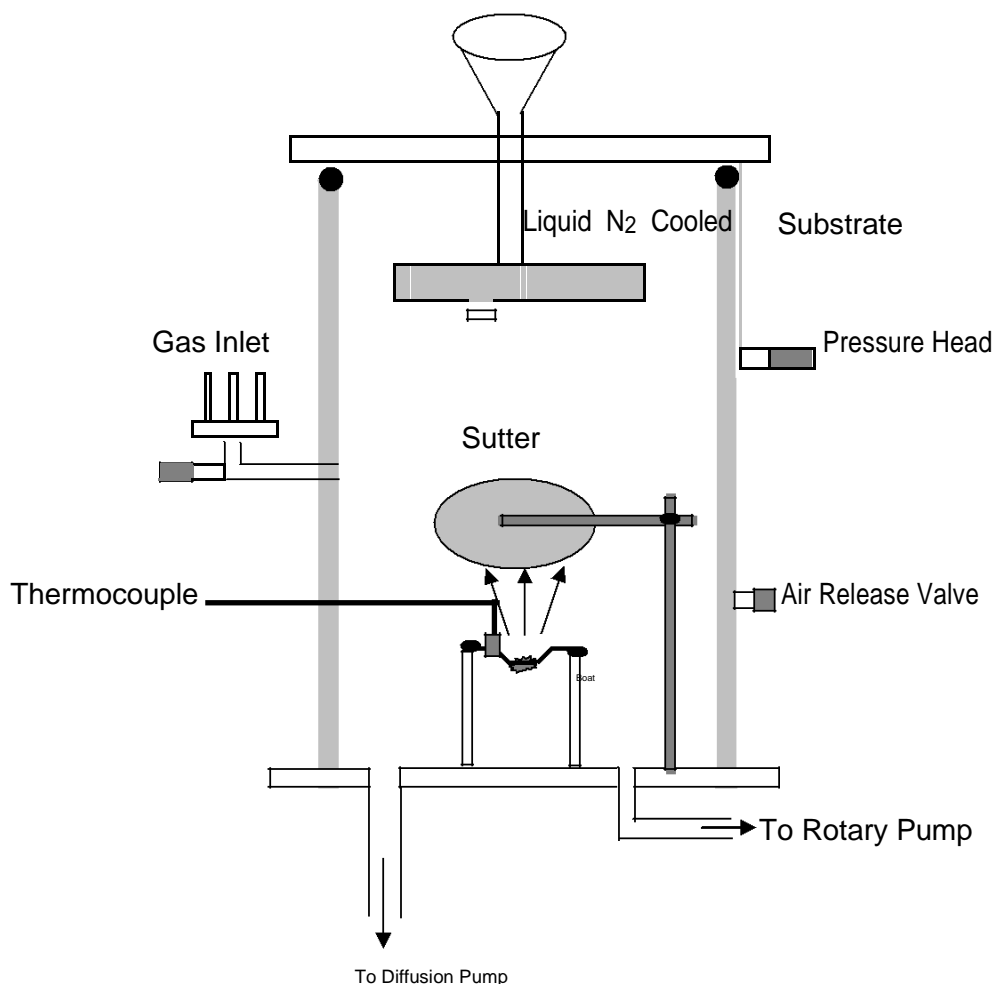


Figure 3.1: Schematic diagram of evaporation chamber

The deposition chamber is mounted over the diffusion pump to maintain vacuum in the deposition chamber. The deposition chamber is cleaned with acetone prior to each deposition. It consists of two copper electrodes. The boat used to evaporate sample consists of an element having very high melting point viz. molybdenum. Molybdenum boat is connected between these two copper electrodes. The argon gas is introduced into the chamber through specially designed inlet tube having a jet of diameter 0.5 mm. This jet is kept adjacent to the evaporation boat pointing towards the glass substrates. The flow of argon gas is controlled by using a needle

valve. The electrodes are connected to a high current, low voltage source to pass high current through the boat. By passing high current, the material present in the boat turned to its molten state and the vapours of the material are formed. These vapours come in contact with inert gas and form clusters. These clusters are transported to the substrates by convectional currents in argon gas. The substrates are kept directly above the boat on a mask at a height of 15 cm from the boat. Before every deposition, the vacuum chamber is evacuated to a vacuum of 10^{-6} mbar using the diffusion pump. The films are deposited on the glass substrate. We have used silicon (100) and quartz substrate for deposition of ZnO thin film. Quartz substrate is used for the optical studies of the grown nanostructures. Powder X-ray diffraction (XRD) is performed using a Philips X-ray diffractometer with $\text{Cu K}\alpha$ (1.54178 \AA) radiation. The morphology and the microstructure of these nanostructures are studied using a Joel field emission scanning electron microscope (FESEM 7500f) and transmission electron microscope (TEM) performed at 100 kV. UV–VIS absorption spectrum is recorded using a V-570 Jasco UV–Vis double-beam spectrophotometer. The scanning wavelength range is 300–900 nm.

3.4 Experimental

Thin film of ZnO is deposited by physical vapour condensation method. In this method, the starting material is Zn powder (99.999 % pure), which is heated at a temperature of 400°C in presence of oxygen and argon gases in the chamber. Initially, small quantity of Zn powder has kept in a molybdenum boat and the chamber has been evacuated to a vacuum of the order of 10^{-6} Torr. After attaining this vacuum, the gases (oxygen and argon) are purged in to the chamber. The pressure of these gases is kept fixed at 16 mbar and 4 mbar respectively. The substrate is cooled with liquid nitrogen and this evaporated material is deposited on glass substrate pasted on this LN_2 cooled substrate. The nanoparticles of ZnO are deposited on the glass substrate and also collected in the powder form by scratching from the substrate. Powder X-ray diffraction (XRD) is performed using a Philips X-ray diffractometer with $\text{Cu K}\alpha$ (1.54178 \AA) radiation. The morphology and the microstructure of these nanostructures are studied using a Joel field emission scanning electron microscope (FESEM 7500f) and TEM performed at 100 kV.

UV–VIS absorption spectrum is recorded using a V-570 Jasco UV–VIS double-beam spectrophotometer. The scanning wavelength range is 300–900 nm. In this experiment, we have successfully grown the ZnO nanostructures at low temperatures, keeping the gases (O_2 and Ar) flow fixed at 6 mbar and 4 mbar respectively. The characterization of semiconducting materials is essential for understanding of their structure, conduction mechanism and for their exploitation in electronic applications. In the present chapter, the various methods and instruments used for the growth and characterization of ZnO nanostructure are described in brief.

3.5 Characterization of ZnO Nanostructures

Electron microscopy takes advantage of the wave nature of rapidly moving electrons. Optical microscopes have their resolution limited by the diffraction of light to about 1000 diameters magnification of around 1,000,000 diameters, primarily because of spherical and chromatic aberrations. The analysis of the structural makeup of ZnO nanostructures is based upon various characterization techniques with the ability to resolve their structure at the nano-scale. Chief amongst these are the TEM, SEM, HRTEM and FESEM, each having their unique

applications. The ZnO thin films are characterized to know about their crystallinity, size, and structure, electrical and optical properties. X-ray diffraction (XRD) gives us good information about structure, size and strain in nanocrystalline materials. Conductivity measurement method is a valuable diagnostic tool for the material quality. It is used to determine the energy distribution of various species of gap states. Optical studies give us good information about band gap and optical transparency of the materials. We also calculated the optical band gap.

3.5.1 X-ray diffraction

X-ray diffraction is a method for identification and quantitative determination of the various crystalline forms of compounds present in powdered and films. In XRD, each atom becomes the source of scattered X-ray radiation. The scattered radiation from all the atoms of amorphous material will combine destructively as they fall on top of one another in the random manner. However, in the case of perfect crystal, the X-rays scatter without the loss of energy and constructive interference may occur. The films of the samples are characterized by using XRD method in the 2θ range from 10° to 70° . Figure 3.2 shows the block diagram of XRD.

X-rays are electromagnetic radiation of wavelength about 1 \AA (10^{-10} m), which is about the same size as an atom. They occur in that portion of the electromagnetic spectrum between gamma-rays and the ultraviolet. The discovery of X-rays in 1895 enabled scientists to probe crystalline structure at the atomic level. When X-rays interact with a crystalline substance (phase), one gets a diffraction pattern. About 95% of all solid materials can be described as crystalline.

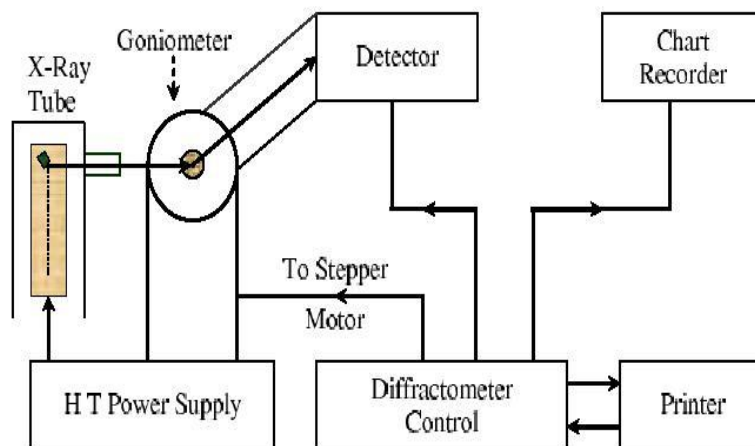


Figure 3.2: Block diagram of X-ray diffraction set up used to study thin film

Each crystalline solid has its unique characteristic X-ray diffraction (XRD) pattern which may be used as a "fingerprint" for its identification. Today about 50,000 inorganic and 25,000 organic single components, crystalline phases, and diffraction patterns have been collected and stored on magnetic or optical media as standards.

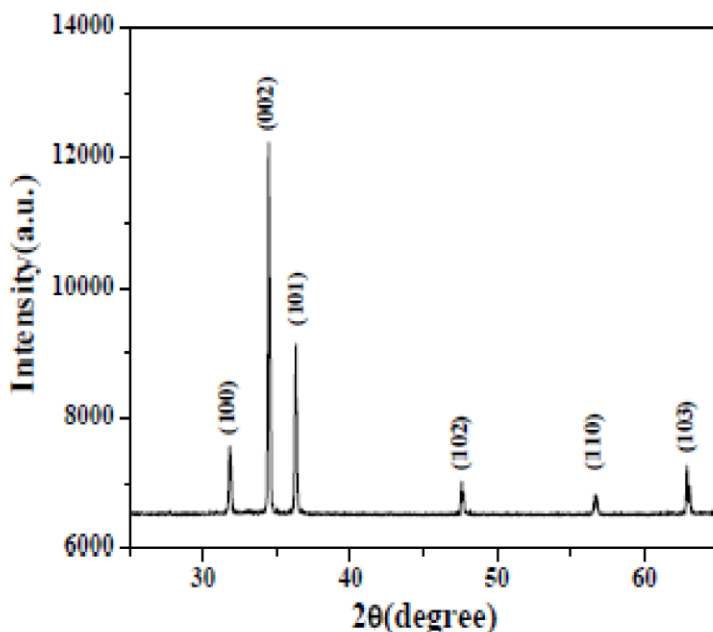


Figure 3.3: Typical XRD pattern of ZnO nanostructures

XRD has been in use in two main areas, for the fingerprint characterization of crystalline materials and the determination of their structure. Once the material has been identified, X-ray crystallography may be used to determine its structure, i.e. how the atoms pack together in the crystalline state and what the interatomic distance and angle are etc. X-ray diffraction is one of the most important characterization tools used in solid state chemistry and materials science. We can determine the size and the shape of the unit cell for any compound most easily using the diffraction of x-rays (Figure 3.3).

3.5.2 Atomic force microscope

The atomic force microscope (AFM) is a very high-resolution type of scanning probe microscope, with demonstrated resolution of fractions of a nanometer, more than 1000 times better than the optical diffraction limit. Binnig, Quate and Gerber invented the first AFM in 1986. The AFM is one of the foremost tools for imaging, measuring and manipulating matter at the nanoscale. The term 'microscope' in the name is actually a misnomer because it implies looking, while in fact the information is gathered by "feeling" the surface with a mechanical probe. Piezoelectric elements that facilitate tiny but accurate and precise movements on (electronic) command enable the very precise scanning. Figure 3.4 illustrates the block diagram of AFM. The AFM consists of a micro scale cantilever with a sharp tip (probe) at its end that is used to scan the specimen surface. The cantilever is typically silicon or silicon nitride with a tip radius of the order of nanometers. The AFM works by scanning a fine ceramic or semiconductor tip over a surface much the same way as a phonograph needle scans a record. When the tip is brought into proximity of a sample surface, Van der Waals forces between the tip and the sample lead to a deflection of the cantilever.

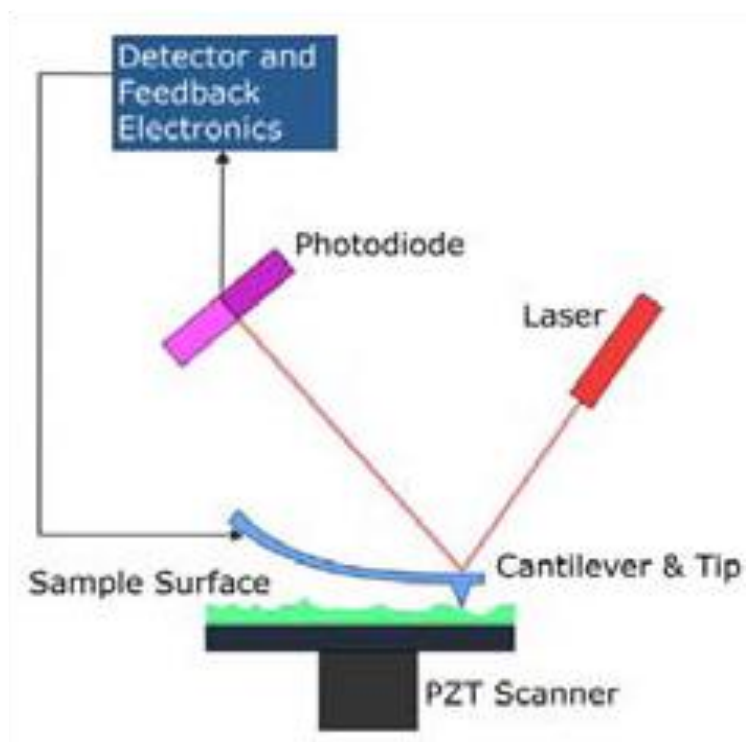


Figure 3.4: Block Diagram of Atomic Force Microscope

The magnitude of the deflection is captured by a laser that reflects at an oblique angle from the very end of the cantilever. A plot of the laser deflection versus tip position on the sample surface provides the resolution of the hills and valleys that constitute the topography of the surface. The AFM can work with the tip touching the sample (contact mode), or the tip can tap across the surface (tapping mode) much like the cane of a blind person.

3.5.3 Transmission Electron Microscope (TEM)

Transmission electron microscopy has been used traditionally as a tool for characterizing local atomic structures of material objects since the information obtained does not require the objects being periodic such as crystal. In the characterization of ZnO nanostructures, TEM is one of the most powerful instruments available due to its excellent imaging and analytical capabilities. TEM imaging allows both the imaging of relatively large areas and the precise measurement of nanostructures diameters. TEM has a very high magnification and can give detailed information about the structure of even a single nanostructure. The nanostructures appear 'transparent' in the TEM pictures, which enables the measurement of both inner and outer diameter. It is also possible to determine the number of layers in a nanostructures tube wall, whether it contains any type of structural damage or irregularities. Another type of interesting observation permitted by the TEM is the shape and location of any residual catalyst that may be incorporated in the tube.

One disadvantage with the TEM is that it has to be manually calibrated by taking pictures of special calibration particles several times during each experimental session. The beads have a known size, which is used to compare and calculate the measurements of the particles in the sample. It can also be argued that the TEM is too powerful to generate a fair interpretation of a nanostructures sample. It is far too tempting to concentrate on details rather than on the general picture. Therefore, a SEM or an optical microscope is likely to give a more accurate overall view than a TEM, except when very short (<100 nm) tubes are present. The inner structure of the as-prepared ZnO nanostructures synthesized by LPCVD was confirmed by TEM.

3.5.4 Scanning Electron Microscope (SEM)

The first scanning electron microscope (SEM) debuted in 1938 (Von Ardenne) with the first commercial instruments around 1965. Its late development was due to the electronics involved in "scanning" the beam of electrons across the sample. SEM is a microscope that uses electrons rather than light to form an image. There are many advantages to using the SEM instead of a light microscope. The SEM has a large depth of field, which allows a large amount of the sample to be in focus at one time. The SEM also produces images of high resolution, which means that closely spaced features can be examined at a high magnification. Preparation of the samples is relatively easy since most SEM only require the sample to be conductive. The combination of higher magnification, larger depth of focus, greater resolution, and ease of sample observation makes the SEM one of the most heavily used instruments in research areas today. The ZnO nanostructures synthesized by LPCVD and ECR-CVD were characterized by SEM.

3.5.5 High Resolution Transmission Electron Microscope

Among various analytical techniques, High-resolution transmission electron microscopy (HRTEM) has played an important role in the discovery and characterization of ZnO nanostructures. It may be claimed that ZnO nanostructures might have not been discovered without using HRTEM. HRTEM has been widely and effectively used for analyzing crystal structures and lattice imperfections in various kinds of advanced materials on an atomic scale. HRTEM images closely depend not only on some optical factors in the imaging process by the electron lens, but also on the scattering process of the electron's incident on the crystal specimen. HRTEM (HRTEM, JOEL-264 JEM3011) confirmed the diameter and inner wall structure of the as-prepared ZnO nanostructures grown by LPCVD and ECR-CVD.

3.5.6 Field Emission Scanning Electron Microscope (FESEM)

A field-emission cathode in the electron gun of a scanning electron microscope provides narrower probing beams at low as well as high electron energy, resulting in both improved spatial resolution and minimized sample charging and damage. Under vacuum, electrons generated by a field emission source are accelerated in a field gradient. The beam passes through electromagnetic lenses, focusing onto the specimen. As a result of this bombardment different types of electrons are emitted from the specimen. A detector catches the secondary electrons and an image of the sample surface is constructed by comparing the intensity of these secondary electrons to the scanning primary electron beam. Finally, the image is displayed on a monitor. The high-resolution reached by FESEM (~ 2 nm) allows the study of very small micro-structural details. FESEM

produces clearer, less electro statically distorted images. By FESEM high quality, low voltage images are obtained with negligible electrical charging of samples. FESEM (FESEM JOEL 6500) measurements have been performed for nano structures synthesized by LPCVD.

3.5.7 Fourier Transform (FT) Raman Spectroscopy

Raman Spectroscopy is a form of vibrational spectroscopy, much like infrared (IR) spectroscopy. It is a powerful, multifaceted technique with wide-ranging applications in carbon nanostructures studies. Raman spectroscopy and Raman spectra allow one to obtain important qualitative and quantitative data. Raman bands arise from a change in the polarizability. The G- D- and G'- bands allow one to examine the diameter and chirality (chiral angle) of carbon nanostructures [15] This may allow one to characterize carbon nanostructures classified as metallic, semi-metallic or semiconducting [16] . It provides deep insight in the physical properties as well as the material quality. It is further used to confirm the graphitic structure of the ZnO nanostructures. Raman spectroscopy (BRUKER, RFS 100/S) was done to confirm the graphitic structure of as-prepared ZnO nanostructures synthesized by LPCVD.

3.6 Optical

Optical characterization of thin film has done by using J. Tauc's method used for materials having direct transition [17, 18]. The glass substrates are used as reference for optical studies. These are having high transparency in the required wavelength range. Figure 3.5 shows the transmission spectrum of substrate used for optical measurements. The transmission spectrum is recorded using computer-controlled Double Beam Scanning NIR/UV/VIS Spectrophotometer [Camspec M550].

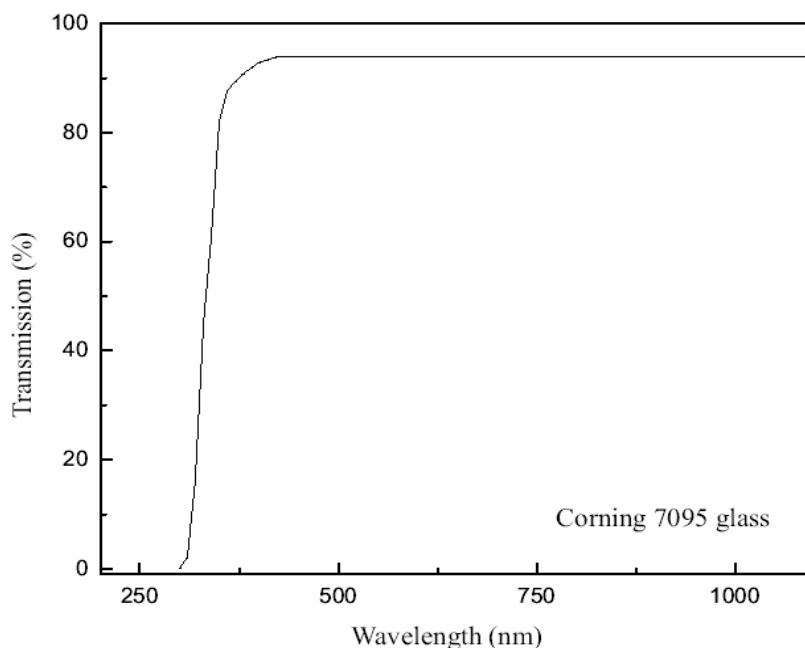


Figure 3.5: Transmission spectrum of glass used for optical studies

3.6.1 UV and IR spectrophotometers

Monochromator spectrophotometer is used to measure the transmission spectrum. Optical layout of monochromator spectrophotometer is shown in Figure 3.6. The light after passing through entrance slit and turning mirror is routed by collimator spherical mirror onto diffraction grating. Grating converts the parallel beam from each point of entrance slit into a fan of monochromatic parallel beams. Camera spherical mirror forms the monochromatic images of these images, when combined, form a spectrum of a certain wavelength range.

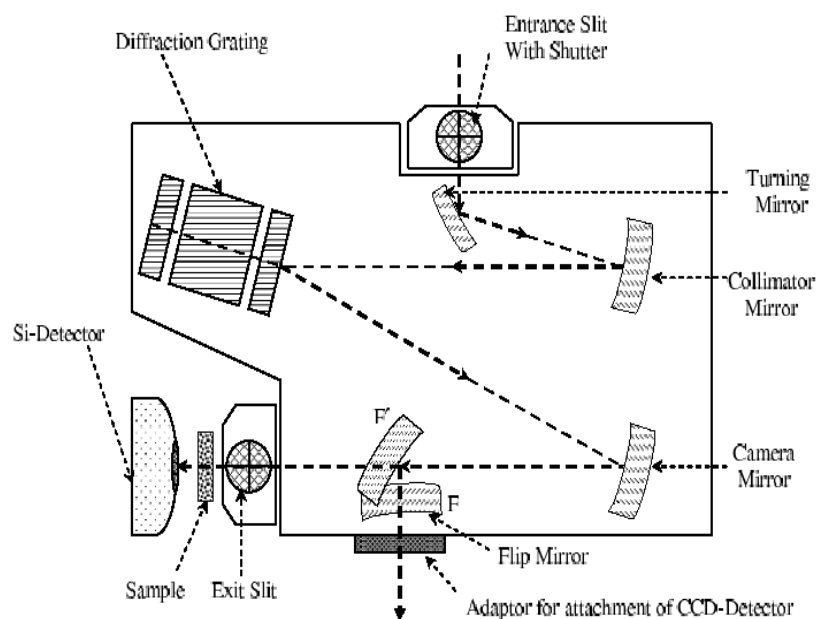


Figure 3.6: Optical layout of monochromator spectrophotometer

The light shutter shuts off the light passing through entrance slit. Diffraction grating is installed on a quadruple turret. The change of diffraction gratings is affected by turning the turret at an angle of 90° around a particular axis. Flip mirror is used for the detector port selection. When the flip mirror is in position F, the axial port is selected as an exit port. When the flip mirror is brought to position F', the lateral port is selected as an exit port. M550 is a completely automated device which uses an internal controller to control the operation of gratings (changeover and rotation), output mirror, entrance/exit slits, filter wheel and shutter. A Si-detector is mounted after the exit slit. The transmittance of the glass substrate with and without film is recorded. The transmission spectra of the film are obtained after subtracting the transmittance of substrate as reference. After passing through the sample compartment, the monochromatic beams are converged and then converted into an electric signal by the detector. The intensities of the two transmitted beams are electronically compared. The electric signal provided from the detector is processed by a CPU and the computational result is displayed directly on the CPU or output to recorder.

3.6.2 Ultraviolet-visible spectroscopy

The spectrophotometers (Figure 3.7) are used in the UV and visible regions of the spectrum and some of these instruments also operate into the near-infrared region as well. Visible region 400-700 nm spectrophotometer is used extensively in colorimetric science. Ink manufacturers, printing companies, textiles vendors, and many more, need the data provided through colorimetric. They usually take readings at every 20 nanometers along the visible region and produce a spectral reflectance curve. These curves can be used to test a new batch of colorant to check if it makes a match to specifications. Traditional visual region spectrophotometers cannot detect if a colorant has fluorescence. This can make it impossible to manage color issues if one or more of the printing inks are fluorescent. Where a colorant contains fluorescence, a bi-spectral fluorescent spectrophotometer is used. There are two major setups for visual spectrum spectrophotometers, d/8 (spherical) and d/45. The names are due to the geometry of the light source, observer and interior of the measurement chamber. Scientists use this machine to measure the amount of compounds in a sample. If the compound is more concentrated more light will be absorbed by the sample; within small ranges, the Beer-Lambert law holds and the absorbance between samples vary with concentration linearly. Samples are usually prepared in cuvettes; depending on the region of interest, they may be constructed of glass, plastic, or quartz. If you pass white light through a coloured substance, some of the light gets absorbed. Some colourless substances also absorb light - but in the ultra-violet region. Since we can't see UV light, we don't notice this absorption. Different substances absorb different wavelengths of light, and this can be used to help to identify the substance, the presence of particular metal ions, for example, or of particular functional groups in organic compounds. The amount of absorption is also dependent on the concentration of the substance if it is in solution. Measurement of the amount of absorption can be used to find concentrations of very dilute solutions. An absorption spectrophotometer measures the way that the light absorbed by a compound varies across the UV and visible spectrum.



Figure 3.7: *The CamSpec M550 Double Beam Scanning UV/Vis Spectrophotometer*

3.6.3 A simple double beam spectrophotometer

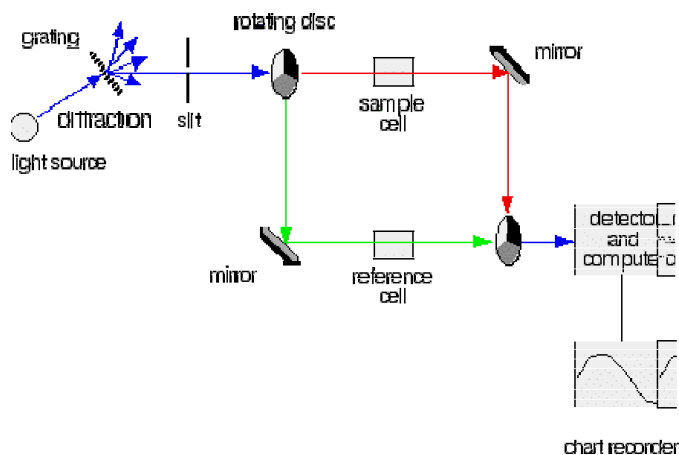


Figure 3.8: Block diagram of simple double beam spectrophotometer

The colour-coding of the light beams through the spectrophotometer is not to show that some light is red or blue or green. The colours are simply to emphasize the two different paths that light can take through the device (Figure 3.8). Where the light is shown as a blue line, this is the path that it will always take. Where it is shown red or green, it will go either one way or the other - depending on how it strikes the rotating disc.

3.7 Electrical properties

Electrical conductivity is a measure of a material's ability to conduct an electric current. When an electrical potential difference is applied across a conductor, its movable charges flow giving rise to an electric current. A conductor such as a metal has high conductivity and a low resistivity. An insulator like glass or a vacuum has low conductivity and a high resistivity. The conductivity of a semiconductor is generally intermediate, but varies widely under different conditions, such as exposure of the material to electric fields or specific frequencies of light, and, most important, with temperature and composition of the semiconductor material. The degree of doping in solid state semiconductors makes a large difference in conductivity. More doping leads to higher conductivity. The conductivity of a solution of water is highly dependent on its concentration of dissolved salts and sometimes other chemical species which tend to ionize in the solution. Electrical conductivity of water samples is used as an indicator of how salt-free, ion-free, or impurity-free the sample is; the purer the water, the lower the conductivity. Electrical conductivity is strongly dependent on temperature. In metals, electrical conductivity decreases with increasing temperature, whereas in semiconductors, electrical conductivity increases with increasing temperature. Over a limited temperature range, the electrical conductivity can be approximated as being directly proportional to temperature. In order to compare electrical conductivity measurements at different temperatures, they need to be standardized to a common temperature. It is well known that there is a strong correlation between structural characteristics of the thin films and their electronic transport properties.

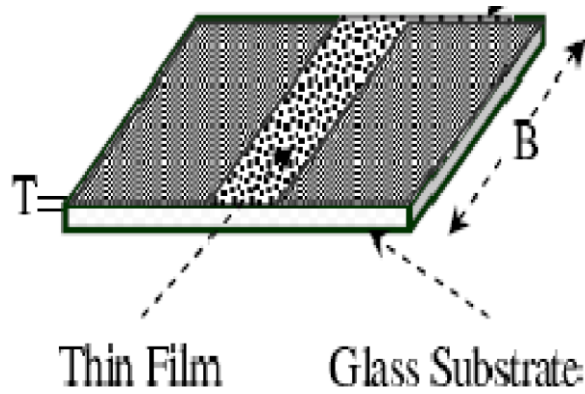
On the other hand, a heat treatment of the films may modify these structural characteristics [19, 20]. Consequently, in situ measurement of some electrical properties such as the electrical resistivity of thin films during their heat treatment may offer very useful information about possible changes in the film structure determined by the heating process [21]. Keeping in mind this assumption, the temperature dependence of the electrical resistivity ρ , during heating of the Zn films has been measured in the temperature range 290–660 K to emphasize the oxidation process. It is known that between the electronic transport properties of polycrystalline semiconducting thin films [22, 23] and their structural characteristics there is a strong correlation. Particularly, both the values and the variation of the electrical conductivity of such films are in connection with their structure and its changes. On the other hand, thermal treatments of the respective films will modify their structural characteristics and consequently, their electrical properties. On this basis, the study of the temperature dependence of the electrical properties of thin films, may offer useful information about the possible changes of the structural characteristics of the films. Moreover, when this study is carried out in situ during successive heating and cooling cycles, such structural changes can be revealed [24–28]. In the case of transparent conducting oxides with applications in optoelectronics (as contact electrodes), the measurements of the electrical resistivity during many successive heating and cooling cycles may provide useful information on the thermal stability of the electrode and temperature limitations.

We consider that the main factor that determines these behaviors of the electrical conductivity is the oxidation process that continues to take place during electrical measurements. Namely, due to the considerable interaction at higher temperature between the remaining Zn amount and atmospheric oxygen, a sharp decrease of the oxygen vacancies which act as shallow donors [29, 30] takes place. The loss of the free charges being irreversible, the electrical conductivity will decrease continuously until the complete oxidation of ZnO films. Also, the evaporation of interstitial Zn atoms due to the higher vapour pressure of zinc [31] can reduce the carrier concentration and hence the electrical conductivity [32] certainly, the structural changes during ZnO film annealing can also influence the carrier mobility, μ , hence the electrical conductivity. But this influence is less pronounced in comparison with that of changes in the stoichiometry of ZnO films [33–37]. On the other hand, the non-linear dependence of the oxygen diffusion rate on the concentration gradient, time and temperature [38] can play an important role in the variation of the electrical conductivity and their irreversibility during the annealing process has been revealed. This behavior is attributed mainly to the oxidation of remaining Zn amount in the films due to the higher heating temperature during electrical measurements. This assumption is sustained by the strong c-axis orientated polycrystalline structures received for both typical two ZnO films after electrical measurements. To study the conduction mechanism in my ZnO films, conductivity measurements are performed at different temperatures for the films prepared by physical vapor deposition method. The calculated conductivity is found to follow the Arrhenius equation:

$$\sigma = \sigma_0 \exp(-E_a/kT) \quad (3.1)$$

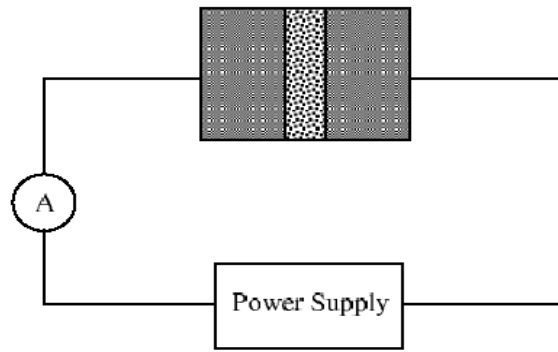
where, σ_0 is a constant, E_a is the activation energy of the electron transport in the conduction band, k is the Boltzmann constant and T is the absolute temperature.

The present measurements are found to be of the same nature in the ZnO thin film deposited in different temperature. Good Ohmic contacts are necessary for any electrical measurement. In the present work, pre-deposited silver electrodes are used for various electrical measurements. Electrodes thick silver electrodes are used for good electrical contacts. The electrodes are deposited using a mask with breadth equal to the side of the substrate and is tied in between so that a gap is left for the deposition of thin ZnO thin film between the electrodes. Thin ZnO thin film of the required samples are deposited on to the electrode gap (using a mask that exposes only the electrode gap of the substrates) by passing low voltage and high current through the Molybdenum boat containing the material. These ZnO thin films of the alloys are used to make the necessary electrical measurements. Figure 3.9 (i) show the silver electrodes, along with the thin film deposited on glass substrate, used for electrical measurements (Figure 3.9- ii). Here L is the length (electrode gap), B is the breadth and T is the thickness of the thin film so that the area of cross-section for current is $A = B \times T$.



(i)

Figure 3.9: (i) Pre-deposited silver electrodes with thin film on glass substrate



(ii)

Figure 3.9: (ii) Setup for electrical measurements

3.7.1 Design of Sample Holder

To carry out the various electrical measurements on the ZnO thin film including both the dc and photoconductivity measurements at low and high temperature, we used a specially designed metallic (stainless steel) sample holder. The detailed diagram of the sample holder is shown in the Figure 3.10. Stainless steel is used to take care of the surface currents and unwanted disturbances in the measurements of small currents [of the order of pico amperes (pA)]. It also helps to provide proper shielding to the thin film samples for accurate current measurements during various experimental observations. At low and high temperatures, stainless steel is highly durable and corrosion-free.

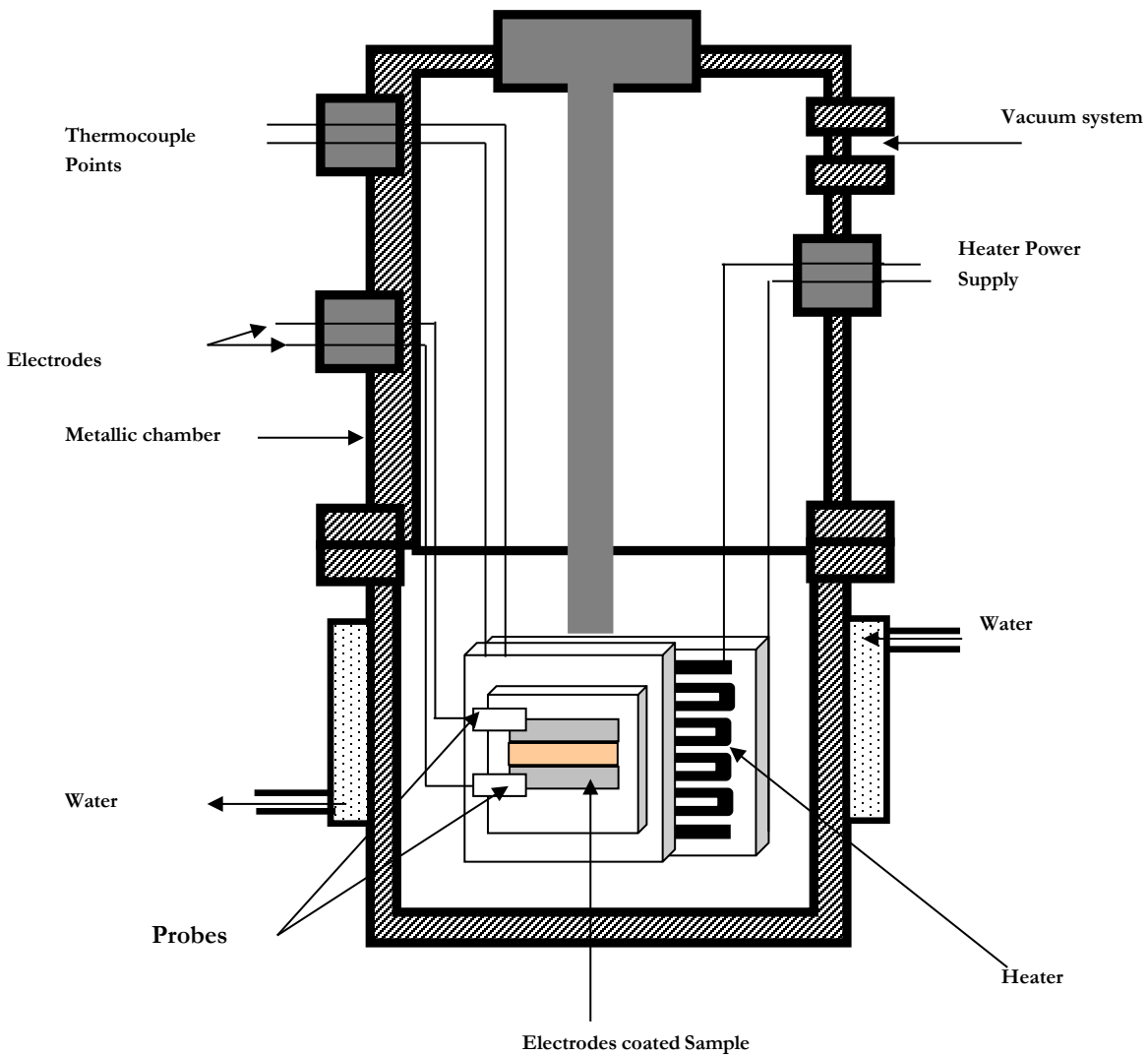


Figure 3.10: Setup for electrical measurements

The sample holder is fitted with a Chromel-Alumel thermocouple using Teflon feed through. During different measurements, this thermocouple gives the exact temperature reading to which the thin film is subjected. The junction of thermocouple is placed on copper block over another glass substrate very near to the thin film so that the chances of error in temperature measurement are very rare. A small circular glass window is installed in the sample holder directly in front of the space at which the film is placed on the copper block. The other end of this copper block is in direct contact with liquid nitrogen. By this arrangement, the temperature gradient is very small between the copper block and the liquid nitrogen filled in the sample holder. The light is shown through a glass window to carry out the photoconductivity measurements on the thin films. To cut off the IR part of light, water in a transparent glass cell is kept in front of the glass window while taking various photoconductivity measurements. The copper block from lower side is fitted with two heaters. These heaters are used to anneal the thin ZnO thin film of various samples and to study their behaviour with rise in temperature. These heaters are connected to a variac using Teflon feed through from outside the sample holder to vary the rate of heating. The rate is monitored through display of the digital panel meter which is connected to the thermocouple. The leakage current in the feed through (BNC connectors) is below the measuring limit (10-12A) of the pico-ammeter used.

3.8 References

- [1] J. Kasai, T. Kitatani, K. Adachi, K. Nakahara and M. Aoki, *Journal of Crystal Growth* 301 (2000) 545.
- [2] M.T. Harrison, S.V. Kershaw, M.G. Burt, A.L. Rogach, A. Kornowski, A. Eychmuller and H. Weller, *Pure Appl. Chem.* 72 (2000) 295.
- [3] F. Zhang, S. Krishnaswamy and C.M. Lilley, *Ultrasonics* 45 (2006) 66
- [4] J. Wu, P. Li, S. Hao, H. Yang and Z. Lan, *Electrochimica Acta* 52 (2007) 5334.
- [5] R.K. Hazra, M. Ghosh and S.P. Bhattacharyya, *Chemical Physics* 333 (2007) 18.
- [6] V. Kovalevskij and V. Gulbinas, *Acta Physica Polonica A* 107 (2005) 351.
- [7] V.M. Lyubin, M. Klebanov, B. Sfez and B. Ashkinadze, *Materials Letters* 58 (2004) 1706.
- [8] A.L. Efros and A.L. Efros, *Sov. Phys. Semicond.* 16 (1982) 772.
- [9] W.P. Halperin, *Rew. Mod. Phys.* 58 (1986) 533.
- [10] A.P. Alivisatos, *Science*, 271 (1996) 933.
- [11] J.C.C. Freitas, E. Nunes, E.C. Passamani, C. Larica, G. Kellermann and A.F. Craievich, *Acta Materialia* 54 (2006) 5095.
- [12] X.W. Wang, G.T. Fei, K. Zheng, Z. Jin and L.D. Zhang, *Appl. Phys. Lett.* 88 (2006) 173114.
- [13] K.K. Nanda, *Chem. Phys. Lett.* 419 (2006) 195.
- [14] M. Li and J.C. Li, *Materials Letters* 60 (2006) 2526.
- [15] R. Saito, G. Dresselhaus and M. S. Dresselhaus, *Physical Properties of carbon Nanotubes*, Imperial College Press, London 1999 synthesis, devices and integrated systems, X. Liu, C. Lee, S. Hua, C. Li and C. Zhou, *Molecular Nanoelectronics*, 2003.
- [15] S. D. E. Lyshevski, *Micro- and nano-electromechanical systems: fundamentals of micro-and nano-engineering*, CRC press , Boca Raton ,FL 2004.
- [16] J. Tauc and A. Menth, *J. Non-Cryst. Sol.* 8 (1972) 569.
- [17] I. Chakraborty and S.P. Moulik, *J. Nanopart. Res.* 7 (2005) 237.

- [18] K.L. Chopra, *Thin Film Phenomena*, Mc. Graw-Hill, New York, 1996.
- [20]. L.L. Kazmerski (Ed.), *Polycrystalline and Amorphous Thin Films*
- [21]. G.G. Rusu, M. Rusu, *Solid State Commun.* 116 (2000) 363.
- [23] G. Harbeke (Ed.), *Polycrystalline Semiconductors: Physical Properties and Applications*, Springer, Berlin, 1985.
- [24] M. Girtan, G.I. Rusu, G.G. Rusu, *Mater. Sci. Eng. B* 76 (2000) 156.
- [25] M. Girtan, G.I. Rusu, G.G. Rusu, S. Gurlui, *Appl. Surf. Sci.* 162–163 (2000) 490.
- [26] G.G. Rusu, *J. Optoelectron. Adv. Mater.* 8 (3) (2006) 931.
- [27] G.G. Rusu, M. Rusu, *Solid State Commun.* 116 (7) (2000) 363.
- [28] M. Girtan, *Surface Coatings Technol.* 184 (2004) 219.
- [29] Z.L. Wang, *J. Phys. Condens. Matter* 16 (2004) R829.
- [30] S. Kohiki, M. Nishitani, T. Wanda, *J. Appl. Phys.* 75 (1994) 2069.
- [31] Y. Igasaki, H. Saito, *J. Appl. Phys.* 69 (1991) 2190.
- [32] A. El Manouni, F.J. Manjon, M. Perales, M. Mollar, B. Mari, M.C. Lopez, J.R. Ramos Barrado, *Superlattice Microst.* 42 (2007) 134.
- [33] G. Epurescu, G. Dinescu, A. Moldovan, R. Birjega, F. Dipietrantonio, E. Verona, P. Verardi, L.C. Nistor, C. Ghica, G. Van Tendeloo, M. Dinescu, *Superlattice Microst.* 42 (2007) 79.
- [34] D. Dimova-Malinovska, H. Nichev, O. Angelov, V. Grigorov, M. Kamenova, *Superlattice Microst.* 42 (2007) 1233.
- [35] B.N. Mukashev, A.B. Aimagambetov, D.M. Mukhamedshina, N.B. Beisenkhanov, K.A. Mit', I.V. Valitova, E.A. Dmitrieva, *Superlattice Microst.* 42 (2007) 103.
- [36] B.N. Mukashev, S.Zh. Tokmoldin, N.B. Beisenkhanov, S.M. Kikkarin, I.V. Valitova, V.B. Glazman, A.B. Aimagambetov, E.A. Dmitrieva, B.M. Veremenithev, *Mater. Sci. Eng. B* 118 (1–3) (2005) 164.
- [37] Ya.I. Alivov, A.V. Chernykh, M.V. Chukichev, R.Y. Korotkov, *Thin Solid Films* 473 (2) (2005) 241.
- [38] H.F. Wolf, *Semiconductors*, Wiley-Interscience, New York, 1971.